A Developmental Switch in the Excitability and Function of the Starburst Network in the Mammalian Retina

Ji-jian Zheng,[1] Seunghoon Lee,[1]
and Z. Jimmy Zhou*
Department of Physiology and Biophysics and
Department of Ophthalmology
University of Arkansas for Medical Sciences
Little Rock, Arkansas 72205

Summary

Dual patch-clamp recording and Ca^{2+} uncaging revealed Ca^{2+}-dependent corelease of ACh and GABA from, and the presence of reciprocal nicotinic and GABAergic synapses between, starburst cells in the perinatal rabbit retina. With maturation, the nicotinic synapses between starburst cells dramatically diminished, whereas the GABAergic synapses remained and changed from excitatory to inhibitory, indicating a coordinated conversion of the starburst network excitability from an early hyperexcitatory to a mature nonepileptic state. We show that this transition allows the starburst cells to use their neurotransmitters for two completely different functions. During early development, the starburst network mediates recurrent excitation and spontaneous retinal waves, which are important for visual system development. After vision begins, starburst cells release GABA in a prolonged and Ca^{2+}-dependent manner and inhibit each other laterally via direct GABAergic synapses, which may be important for visual integration, such as the detection of motion direction.

Introduction

During development, many neural networks are highly excitable due to the early excitatory actions of GABA and glycine (Ben-Ari, 2002). These early networks often generate spontaneous bursts of excitation, which are important for activity-dependent neural development (Katz and Shatz, 1996). As development proceeds, ionotropic actions of GABA and glycine change from excitation to inhibition by a delayed expression of chloride exporters (Rivera et al., 1999), thereby providing stability to the network so that the mature form of network processing can occur without epileptic seizures.

In the developing mammalian retina, the early spontaneous wave of excitation relies on nicotinic neurotransmission (Feller et al., 1996). It has been proposed that the cholinergic network formed by starburst amacrine cells is responsible for the generation and propagation of this recurrent retinal excitation (Feller et al., 1997). However, although starburst cells have been shown to directly participate in retinal waves (Zhou, 1998), two essential and puzzling issues remain unsolved. First, we do not know what drives the starburst cell network to burst during retinal waves, and more importantly, there

has been no direct evidence that starburst cells form a mutually excitatory network capable of supporting recurrent excitation. Second, it is not clear how such an intrinsically unstable network, if it exists, could be compatible with mature visual function, since the nicotinic synapses so far studied in the CNS always remain excitatory as the network matures.

Starburst cells are the only neurons in the nervous system known to synthesize both ACh and GABA (Brecha et al., 1988; Kosaka et al., 1988; Vaney and Young, 1988). They have been shown by autoradiography to release ACh and GABA via a Ca^{2+}-dependent vesicular and a Ca^{2+}-independent transporter mechanism, respectively (O'Malley and Masland, 1989; O'Malley et al., 1992). However, the functional role of ACh and GABA release by starburst cells is poorly understood, in part because neither the corelease of ACh and GABA nor the mechanism of release has been studied at a cellular or synaptic level. Unlike most retinal neurons, which tile the retina with little dendritic overlap within the same cell population (Wassle and Boycott, 1991; MacNeil et al., 1999; Rockhill et al., 2000, 2002), starburst cells overlap as much as 70-fold, and their dendrites cofasciculate precisely to form a honeycomb-like network (Tauchi and Masland, 1984; Vaney, 1984; Famiglietti, 1985), raising the intriguing possibility of massive reciprocal synaptic interactions within a network formed by a single population of neurons. Such a network may mediate not only spontaneous retinal waves during development, but also important network computation during mature visual processing, particularly the detection of motion direction, because starburst cells are believed to provide essential inhibition to direction-selective (DS) ganglion cells (Yoshida et al., 2001; Amthor et al., 2002; Euler et al., 2002; Fried et al., 2002; Taylor and Vaney, 2003). A key question regarding the function of mature starburst cells and the DS mechanism is whether the essential GABAergic synaptic inhibition also exists at a level presynaptic to DS ganglion cells, especially among starburst cells.

The goal of this study is to determine (1) whether and how ACh and GABA are coreleased synaptically by a single starburst cell, (2) whether developing starburst cells form a mutually excitatory network to mediate retinal waves, (3) how such a network, if it exists, remains stable (nonepileptic) in the mature retina, and (4) whether GABAergic lateral inhibition occurs within the starburst network during visual processing.

Results

Reciprocal Synaptic Corelease of ACh and GABA by Starburst Cells

Dual whole-cell patch-clamp recordings were made from starburst cell pairs in the ganglion cell layer (GCL) of the whole-mount rabbit retina. The initial recordings focused on perinatal rabbits aged embryonic day 29 to postnatal day 1 (E29–P1; gestation period, 31 days). At this age, starburst cells already attained a distinctive
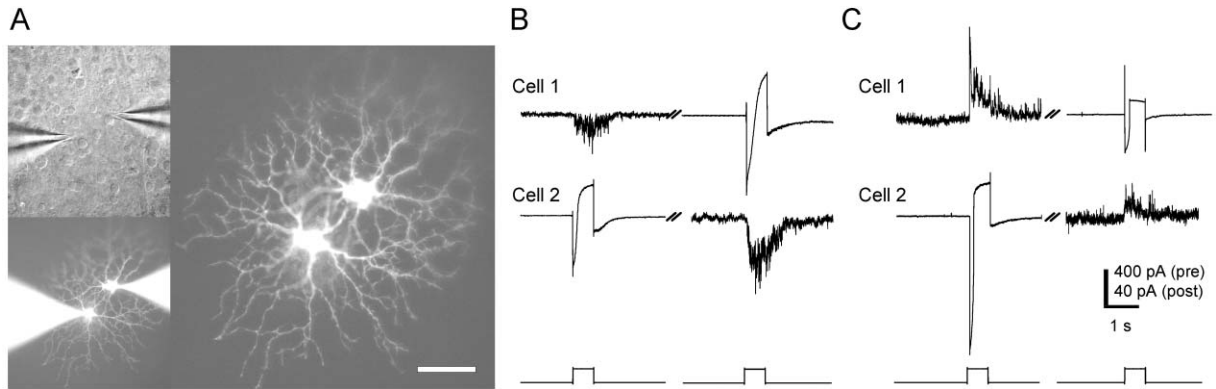
Figure 1. Dual Patch-Clamp Recording from a Pair of Starburst Cells in an E30 Retina

(A) Photomicrographs of a pair of starburst cells recorded with Lucifer yellow-filled patch pipettes viewed with DIC optics (upper left) and epifluorescence (lower left). (Right) Fluorescence image of the same cell pair after the removal of pipettes. Scale bar, 50 μm.

(B) Paired voltage-clamp recording, showing reciprocal synaptic responses ($V_h = -70$mV, postsynaptic) evoked by presynaptic depolarization pulses (from -70 to 0 mV, bottom trace).

(C) Voltage-clamp recording from another E30 starburst pair, showing reciprocal synaptic responses ($V_h = +45$ mV, postsynaptic) evoked by the same presynaptic depolarization pulses (from -70 to 0 mV, bottom trace).

"starburst" morphology (Figure 1A). Paired voltage-clamp recordings revealed synaptic transmission between starburst cells (n = 120 pairs). As shown in Figure 1B, depolarizing one starburst cell (cell 2) from -70 to 0 mV elicited voltage-gated currents in the same cell and inward postsynaptic currents in the other (cell 1, held at -70 mV). The synaptic transmission was often reciprocal (Figure 1B), indicating mutual synaptic communication within the starburst network. For simplicity, we term the cell being induced to release transmitters "presynaptic" and the other cell in the pair "postsynaptic." Figure 1C shows that when the postsynaptic starburst cell was held at $+45$ mV, robust outward synaptic currents were also detected in a reciprocal manner.

To determine whether ACh and GABA were corel eased by a single starburst cell at the synaptic level, we first examined the biophysical and pharmacological properties of the postsynaptic responses. Figure 2A gives an example of dual voltage-clamp recording from a pair of E30 starburst cells, showing inward postsynaptic currents at a holding potential of -70 mV and outward postsynaptic currents at $+45$ mV from the same cell. The inward postsynaptic currents at -70 mV (E_{Cl}) could be completely blocked by the nicotinic antagonist hexamethonium (Hex, 100 μM, n = 5) (Figure 2B) but were not affected by picrotoxin (Pic, 100 μM, n = 4, data not shown), suggesting that they were mediated by nicotinic receptors. On the other hand, the outward postsynaptic currents recorded at $+45$ mV were completely blocked by Pic (100 μM, n = 3, Figure 2B) or the GABA$_A$ antagonist SR95531 (50 μM, n = 3) but not by Hex (100 μM, n = 3), indicating GABA$_A$ receptor-mediated currents.

To confirm the presence of both nicotinic and GABA$_A$ components in the synaptic transmission between starburst cells, we puffed ACh and GABA directly on voltage-clamped starburst cells in perinatal retinas in the presence of 0.3–1 mM Cd^{2+}, which blocked Ca^{2+}-dependent synaptic transmission. Puffing ACh (1 mM) evoked robust, inward-rectifying currents (n = 12) that could be blocked by Hex (100 μM, n = 3, Figures 2C and 2D) but

not by α-bungarotoxin (α-BgTX, 200 nM, n = 2) (Figure 2C), demonstrating the presence of functional, α-bungarotoxin-insensitive nicotinic receptors on these starburst cells. Puffing GABA (1 mM) on starburst cells (n = 8) also elicited robust current responses (Figures 2E and 2F), which were completely blocked by SR-95531 (50 μM, n = 4) or Pic (100 μM, n = 2) and had a nearly liner I-V relation with a reversal potential near the calculated E_{Cl} (-70 mV) (Figures 2E and 2F), indicating the presence of functional GABA$_A$ receptors. Taken together, the above results established that the inward postsynaptic currents recorded at around -70 mV were nicotinic currents and that the outward postsynaptic currents at $+45$ mV were mediated by GABA$_A$ receptors. Hence, these data demonstrated that a single starburst cell released both ACh and GABA at a synaptic level and that the early developing starburst cells formed a network connected by reciprocal nicotinic and GABAergic synapses.

A Developmental Switch in Network Excitability Caused by a Dramatic Reduction in Nicotinic Synaptic Communication among Starburst Cells

To determine how the starburst network acquired the stability necessary for visual processing as the retina matured, we examined the developmental profile of nicotinic synapses between starburst cells by measuring synaptic transmission between and functional nicotinic receptor expression on starburst cells at various developmental stages. Remarkably, we found that the nicotinic synaptic interaction between starburst cells could be detected only during early development and diminished quickly during the first postnatal week. As shown in Figures 3A1–3A3, recording from starburst cell pairs detected both nicotinic (at -70 mV) and GABA$_A$ (at $+45$ mV) synaptic currents at E30, but only GABA responses at P21. In fact, nicotinic postsynaptic responses were never detected between starburst cells after P11 (n = 60), whereas GABA$_A$ receptor-mediated postsynaptic currents persisted throughout development (E29–P31,
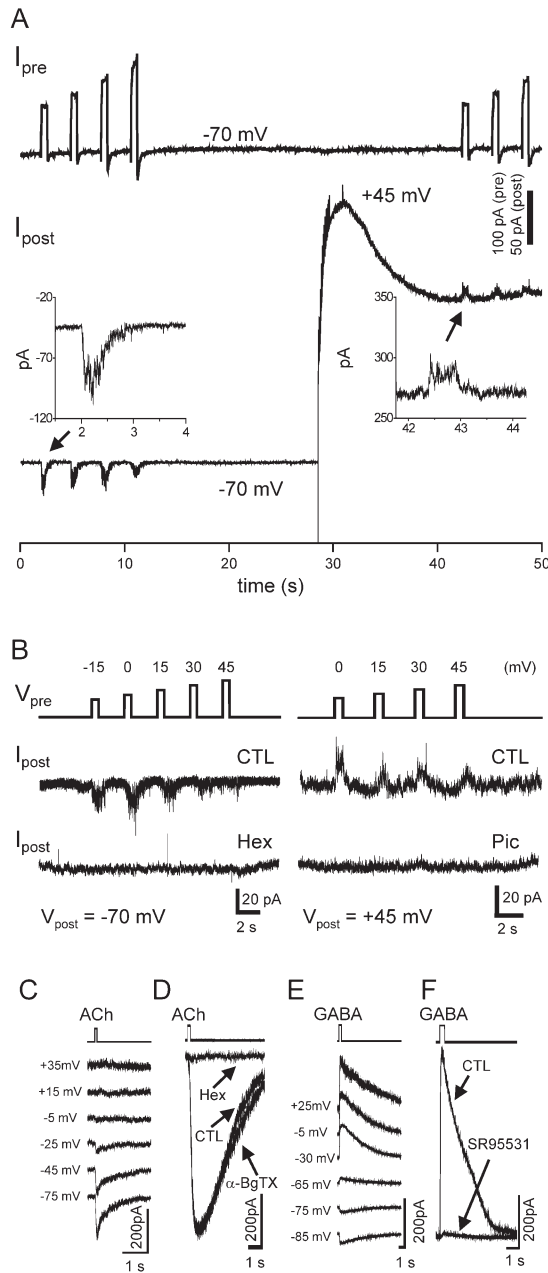
Figure 2. Corelease of ACh and GABA by Starburst Cells in E30 Rabbits

(A) Simultaneous recording of presynaptic voltage-gated currents (I_{pre}) activated by 600 ms long depolarizing pulses (55 mV initial amplitude, 15 mV increments) and postsynaptic currents (I_{post}) from a pair of E30 starburst cells, showing inward postsynaptic currents at $V_h = -70$ mV and outward postsynaptic currents at $V_h = +45$ mV. (Insets) Expanded views of postsynaptic currents marked by arrows.
(B) Recordings from two different pairs of starburst cells, showing a complete blockade of postsynaptic currents at $V_h = -70$ mV by hexamethonium (Hex, 100 μM) (left) and at $V_h = +45$ mV by picrotoxin (Pic, 100 μM) (right).
(C) Current responses of a starburst cell to puffs of ACh (1 mM) in the presence of 0.5 mM Cd^{2+}, showing a completely inward-rectifying current-voltage relation.
(D) The ACh-evoked current (recorded from another cell at -70 mV) was Hex (100 μM) sensitive and α-bungarotoxin (200 nM) insensitive.
(E) Puffing GABA (1 mM) in the presence of 0.5 mM Cd^{2+} evoked

n = 70). Similarly, puffing ACh (1 mM) onto starburst cells evoked robust nicotinic currents at E30, but little responses at P21 (Figure 3C). In contrast, the response of starburst cells to the GABA puff persisted as the retina matured (Figure 3C). A quantitative assessment of the starburst responses to ACh puffs (1 mM) revealed a dramatic postnatal decline in the peak nicotinic response amplitude, from an average value of 1450 ± 210 pA at E29 to 97 ± 14 pA at eye opening (P11, n = 3), and was nearly undetectable (5 ± 5 pA) at P28 (n = 3) (Figure 3B). This drastic reduction in the response amplitude to an ACh puff could not be explained by the developmental enhancement of the cholinesterase activity in the mammalian retina (Hutchins et al., 1995), because a similar reduction was also found when cholinesterase was inhibited by neostigmine (NS, 4 μM), even though NS did increase the ACh response amplitude from 1140 ± 180 pA to 1280 ± 300 at E30 (n = 3) and from 11 ± 5 pA to 41 ± 7 pA at P25 (n = 4). Similarly, the response amplitude to a puff of the nonhydrolizable nicotinic agonist 1.1-dimethyl-4-phenyl piperazinium iodide (DMPP) (1 mM) also declined drastically from 2070 ± 16 pA (n = 3) at E29 to 47 ± 8 pA at P26 (n = 3) and 29 ± 9 pA in adult (n = 3, Figure 3D). This striking developmental decline in nicotinic synaptic transmission between starburst cells is indicative of a programmed elimination of the early form of massive cholinergic connections among starburst cells, suggesting an important switch in the starburst network excitability.

The above switch in the starburst network excitability was accompanied by pronounced changes in starburst morphology. As shown in Figure 3E, perinatal starburst processes consisted of numerous filopodia but few varicosities. Interestingly, these filopodia also disappeared during postnatal development, with a time course (Wong and Collin, 1989) similar to that shown in Figure 3B, suggesting a possible link between this morphological change and the transitions in the network excitability and synaptic connectivity. As the retina matured, numerous varicosities appeared on distal starburst processes (Figure 3E), which are believed to be the neurotransmitter release sites in adult (Famiglietti, 1991).

Functional Roles of the Changing Starburst Network Excitability
To gain an insight into the functional consequences of the developmental changes in starburst excitability, we investigated the role of starburst-starburst interactions at three developmental stages: around birth (E29–P1), during the decline of nicotinic responses (P3–P8), and after eye opening (P11–P29).

As described in the Introduction, in order to prove the hypothesis (Feller et al., 1997; Feller, 1999; O'Donovan, 1999) that recurrent excitation in the starburst system mediates early spontaneous retinal waves, two critical questions need to be answered. First, do starburst cells actually form a mutually excitatory network? Second, what drives starburst cells during the wave? With dual

robust currents that reversed at $\sim$$E_{Cl}$ (-69 mV).
(F) The response to GABA (from another cell, at $+45$ mV) was blocked by SR95531 (50 μM).
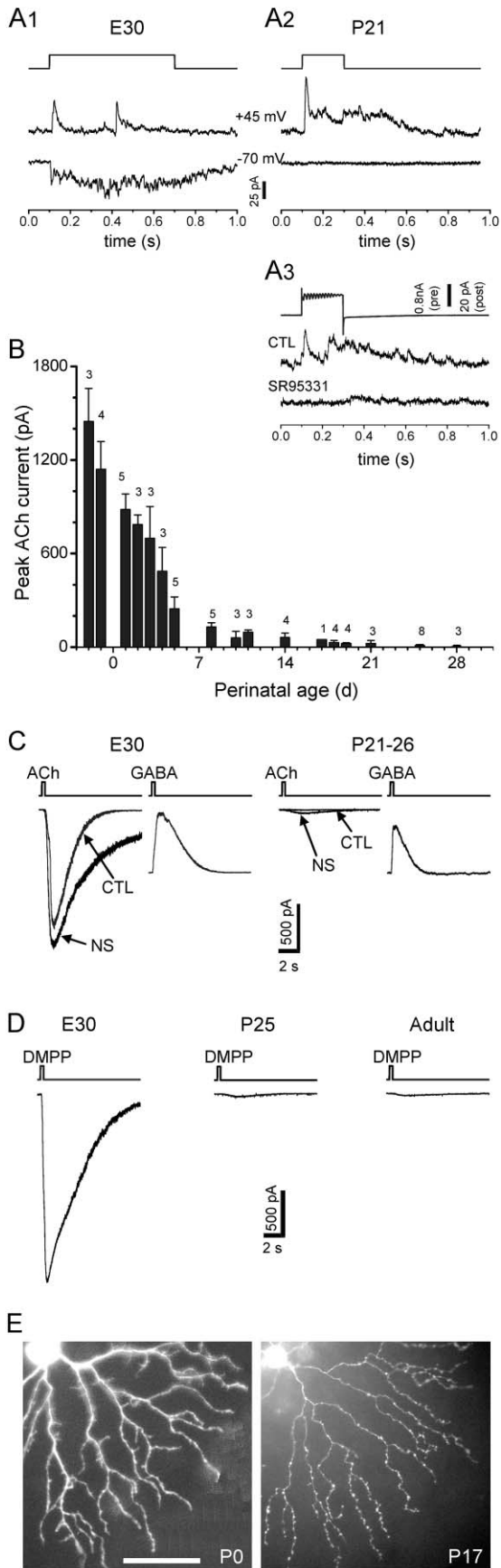
patch-clamp recording, we now directly demonstrated reciprocal nicotinic interactions between perinatal starburst cells (Figure 4A1), thus proving the existence of a recurrent cholinergic network. To determine what synaptic inputs starburst cells received during the wave, we examined the physiological and pharmacological properties of the bursting synaptic currents in starburst cells during early retinal waves. Figure 4A2 shows bursts of synaptic currents in a pair of starburst cells voltage clamped at +45 mV and −70 mV, respectively. Pic (100 μM) completely blocked the outward currents at +45 mV, but did not affect the rhythmic inward currents at −70 mV (Figure 4A2, n = 6) or the retinal waves under Ca^{2+} imaging (n = 12, data not shown), suggesting that the ionotropic GABA input, though significant, was not an essential component of the synaptic drive responsible for the waves. However, Hex (100 μM), applied either alone (n = 5, data not shown) or together with Pic (n = 3, Figure 4A2), completely and reversibly blocked all rhythmic currents in starburst cells, suggesting that nicotinic inputs were associated with the waves. Hence, during early spontaneous retinal waves, the starburst network was driven synaptically by the mutual excitation among starburst cells themselves, but not by an external system. This result was confirmed by the finding that glutamate receptor antagonists CNQX (40 μM) and AP7 (200 μM) did not have any effect on the synaptic currents (either inward or outward) in starburst cell during the waves (Figure 4A3, n = 4). Together, these data provide strong physiological evidence for the theory that recurrent excitation within the starburst network mediates the early spontaneous retinal waves.

Figure 3. Developmental Transitions in Starburst Cell Excitability and Dendritic Structure

(A1) Dual patch-clamp recording from a pair of E30 starburst cells, showing both outward (V_h = +45 mV) and inward (V_h = −70 mV) postsynaptic currents in response to a voltage step (−70 to 0 mV, top trace) applied to the presynaptic starburst cell.

(A2) Similar recordings from a pair of P21 starburst cells detected outward postsynaptic currents (V_h = +45 mV) but no inward currents (V_h = −70 mV). Recordings were made in the presence of 40 μM CNQX to block spontaneous glutamate currents.

(A3) Paired recording from a P17 starburst pair (in 40 μM CNQX), showing voltage-gated currents (in the presynaptic cell) elicited by a voltage step from −70 mV to +10 mV (top trace) and outward postsynaptic currents at V_h = +45 mV (middle trace), which was completely blocked by the $GABA_A$-selective antagonist SR95531 (50 μM, bottom trace, n = 5).

(B) Age-dependent decline of peak current responses of starburst cells to ACh puffs (1 mM) in the presence of 0.5–1 mM Cd^{2+}. The numbers of cells tested are shown above the histogram. Error bars, standard deviation.

(C) Representative responses (at V_h = −70 mV) of an E30 and a P26 starburst cell to an ACh (1 mM) puff in the control solution and in the presence of neostigmine (NS, 4 μM). Representative responses (at V_h = + 40 mV) of an E30 and a P21 starburst cell to a GABA (1 mM) puff are shown for comparison. The control solution contained 1–2 mM Cd^{2+}.

(D) Representative responses of E30, P25, and adult starburst cells to DMPP puffs (1 mM) recorded in the presence of 1 mM Cd^{2+} at −70 mV.

(E) Comparison between the dendritic morphology (only one quadrant of the dendritic tree is shown) of a P0 and a P17 starburst cell following whole-cell patch clamp with Lucifer yellow-filled pipettes, showing prominent dendritic filopodia at P0 and numerous varicosities in distal dendrites at P17. Scale bar, 50 μm.

Similar pharmacological analysis of P4–8 starburst cells showed that the inputs to starburst cells during the late-stage retinal wave were insensitive to nicotinic antagonists (Figure 4B1, n = 4), but could be reversibly blocked by CNQX and AP7 (Figure 4B2, n = 5), consistent with the pharmacology of retinal waves measured by Ca^{2+} imaging at this stage (Zhou and Zhao, 2000). Pic (100 μM) greatly enhanced both spontaneous bursts in starburst cells (Figure 4B1) and the Ca^{2+} waves in the retina (Zhou, 2001), indicating an inhibitory action of the GABA inputs at this age. To determine when $GABA_A$ input to starburst cells changed from excitatory to inhibitory, we puffed the $GABA_A$ agonist muscimol (1 mM) on Fura-2AM-loaded starburst cells in the presence of Hex (200 μM), CNQX (40 μM), and AP7 (100 μM), which would block indirect effects mediated by nicotinic and glutamate receptors. Muscimol puffs evoked a Ca^{2+} rise in E29 starburst cells, an effect that was blocked by 40 μM SR95531 (n = 4, data not shown). However, muscimol puffs under the same condition did not elicit any detectable Ca^{2+} rise in P5 starburst cells (n = 5), suggesting that $GABA_A$ input to starburst cells changed from excitatory to inhibitory between E29 and P5, presumably due to an increased KCC2 expression (Vu et al., 2000). Together, these results showed that the dramatic decline of nicotinic responses of starburst cells (Figure 3B) followed the same time course as that of the transition from a nicotinic to a glutamatergic mechanism of retinal waves (Zhou and Zhao, 2000), and it was also concomitant with the emergence of a strong inhibitory ionotropic GABA action on the waves (Figure 4B1) (Zhou and Zhao, 2000). Importantly, this finding resolved a long-standing puzzle as to why nicotinic interactions were no longer involved in late retinal waves.

After eye opening (>P11), starburst cells are believed to mediate important visual processing in the retina, especially directional selectivity; however, essentially nothing is known about any physiological interaction among starburst cells. Using dual patch clamp, we found in P11–P29 rabbits that starburst cells directly communicated with each other via reciprocal $GABA_A$ synapses (Figure 4C1). In the 40 pairs of starburst cells (>P15) that showed GABAergic synaptic transmission, 30 pairs were found to have reciprocal synaptic interactions (the actual number of reciprocal pairs is expected to be higher than 30, because sometimes Ca^{2+} channels and other intracellular factors might have run down before the second cell in the pair was tested for synaptic release). Thus, we believe most mature starburst cells were reciprocally connected by $GABA_A$ synapses. We also detected, in the presence of 2 μM strychnine, light-evoked synaptic currents in starburst cells (V_h = −5 mV, E_{cation}, Figure 4C2, n = 20), which were outward and SR95531 sensitive, indicating that $GABA_A$ receptors on starburst cells mediated light-evoked inhibition. Because of the presence of direct GABAergic synapses between starburst cells (Figures 3A2, 3A3, and 4C1), a significant part of this light-evoked GABAergic inhibition must have come from neighboring starburst cells, even though other GABAergic amacrine cell types might also have a contribution. To directly demonstrate this idea, we examined the contribution of a single starburst cell (cell 2, voltage clamped at −70 mV, Figures 4D1–4D3) to the light response of a neighboring starburst cell (cell

1, voltage clamped at −15 mV, Figures 4D1–4D3). We first established that depolarizing cell 2 with a voltage step (−70 to 0 mV) produced an inhibitory (outward) current in cell 1 (Figure 4D1). We then used a 100 μm diameter center spot illumination to stimulate both cells, evoking in cell 1 an initial inward excitatory current (presumably mediated by glutamate), followed by an outward inhibitory current (Figure 4D2). We next gave the light flash simultaneously with the voltage step (−70 to 0 mV, to cell 2 only). As shown in Figure 4D3, because of the voltage step-evoked inhibitory input from cell 2 to cell 1, the light response of cell 1 was shifted outward. Under this recording condition, the inhibition was quite effective (nearly completely canceling out the light-evoked inward current in cell 1), because the inhibitory input from cell 2 to cell 1 arrived earlier than did the light-evoked inward (excitatory) currents in cell 1 (Figure 4D3). This experiment, though done under special stimulation conditions to reveal otherwise undetectable current components, directly demonstrated the inhibitory contribution of a single starburst cell to the light response properties of its neighboring starburst cells. This inhibition may also produce a voltage shunting near the resting membrane potential of starburst cells.

Direct lateral inhibition between starburst cells may play an important role in direction selectivity (see Discussion). Because retinal light response properties in P21 rabbits are essentially the same as those in adult (Masland, 1977), the synaptic physiology we characterized in P21–P29 starburst cells is expected to be very similar to that in adult. Patch-clamp recording from ON-OFF DS ganglion cells also revealed strongly direction-selective light responses as well as direction-selective GABAergic and glutamatergic inputs to DS ganglion cells at eye opening (S.L. and Z.J.Z., unpublished data), indicating the presence of a functional DS network, including a preganglionic DS inhibitory circuit involving starburst cells well before P21.

Mechanisms of ACh and GABA Release by Starburst Cells

We next examined whether synaptic releases of ACh and GABA from starburst processes were mediated by a Ca^{2+}-dependent vesicular mechanism or by Ca^{2+}-independent transporters. Application of 500 μM Cd^{2+} during paired recordings completely blocked both presynaptic voltage-gated Ca^{2+} currents and Ca^{2+}-activated currents and postsynaptic nicotinic (n = 3 pairs, E29–P0, Figure 5A1) and $GABA_A$ currents in perinatal starburst cells (n = 3 pairs, E30, Figure 5A2), suggesting a dependence of both ACh and GABA releases on Ca^{2+} entry through voltage-gated Ca^{2+} channels. Cd^{2+} (500 μM) also blocked $GABA_A$-mediated synaptic transmission between starburst cells in P18–P29 rabbits (n = 3) (Figure 5B). Figure 5C shows the relationship between presynaptic depolarization and postsynaptic ACh (E29) and GABA (P21) currents. The threshold for both ACh (E29–P1) and GABA (E29–P29) release was variable (between −50 and −20 mV), likely due to the variability in the size of detectable postsynaptic currents, the number and location of synaptic contacts and other experimental conditions.

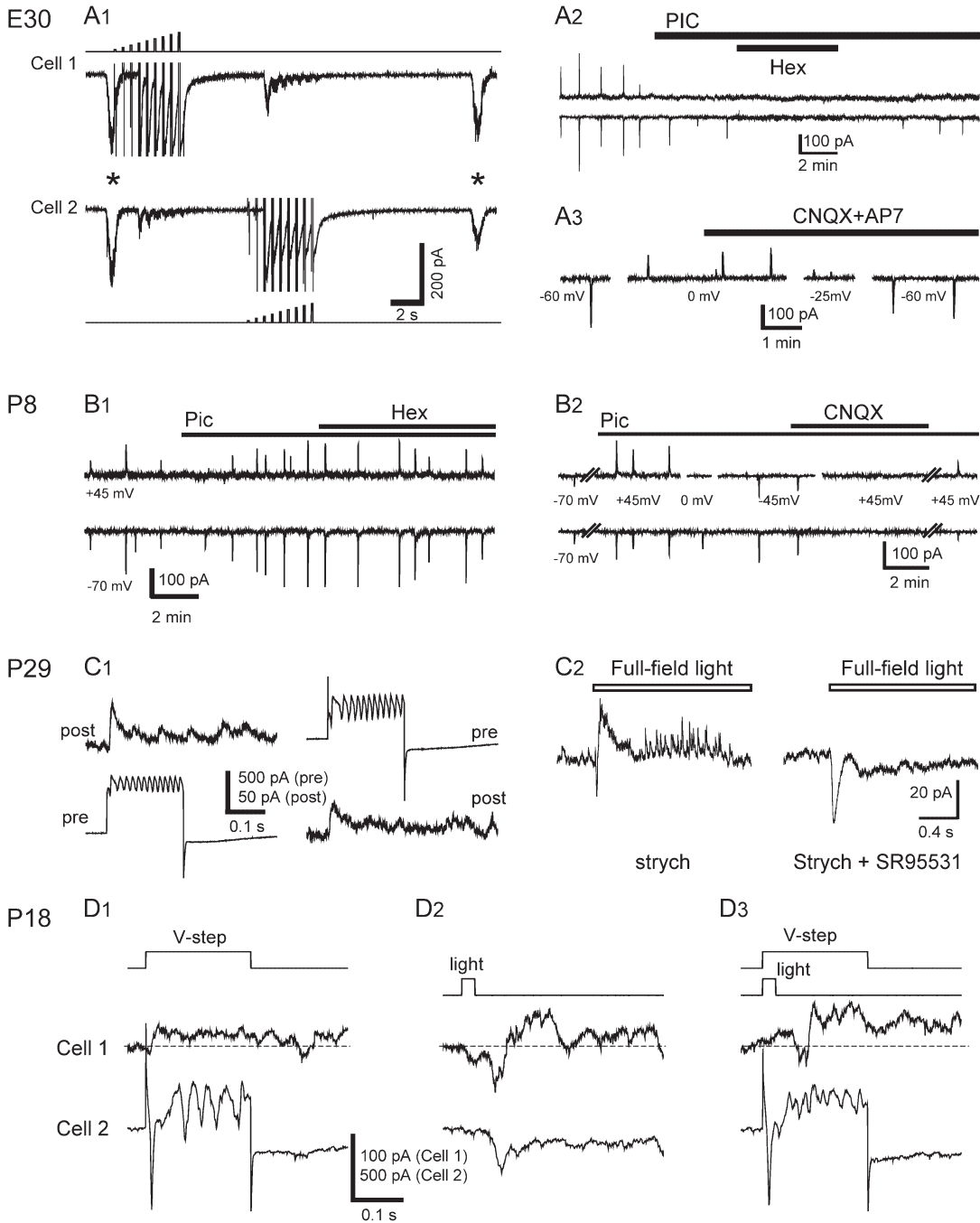To further demonstrate that a Ca^{2+} increase alone,

Figure 4. Developmental Transitions in Starburst Network Function

(A1–A3) Nicotinic synapses between starburst cells mediate early retinal waves. (A1) Comparison between spontaneous synaptic inputs during retinal waves (asterisks) and reciprocal synaptic currents evoked by voltage pulses (in 10 mV increments, top and bottom traces) from an E30 starburst cell pair ($V_h = -70$ mV). (A2) Rhythmic spontaneous currents in a pair of E30 starburst cells ($V_h = -70$ and $+45$ mV, respectively). Picrotoxin (Pic, 100 μM) blocked the outward currents at $+45$ mV, but not the inward currents at -70 mV. Addition of hexamethonium (Hex, 100 μM) completely and reversibly blocked the spontaneous currents. (A3) Continuous voltage-clamp recording (at four different potentials) of an E30 starburst cell, showing a lack of effect of 40 μM CNQX + 200 μM AP7.

(B1 and B2) Transition from a nicotinic to a glutamatergic drive for retinal waves. (B1) Spontaneous rhythmic currents from a pair of P8 starburst cells ($V_h = +45$ and -70 mV, respectively), showing an enhancement of the currents by Pic (100 μM) and a lack of effect of Hex (100 μM). (B2) Rhythmic currents in another P8 starburst cell pair were enhanced by Pic (100 μM) and reversibly blocked by CNQX (25 μM). (C and D) GABAergic inhibition of starburst cell light responses after eye opening. (C1) Reciprocal GABAergic currents ($V_h = +45$ mV) from a pair of P29 starburst cells in response to presynaptic depolarization (-70 to 0 mV). (The oscillating currents in the presynaptic cells were sensitive to TEA and Cd^{2+}, data not shown.) (C2) (Left) responses to a full-field light stimulus from the same starburst cell as in (C1) (upper) ($V_h = -5$ mV) in the presence of 2 μM strychnine, showing a brief inward current at the light onset, followed by repetitive outward synaptic currents. (Right) SR95531 (50 μM) abolished the outward currents and increased the amplitude and duration of the initial inward response

without presynaptic depolarization (which might activate GABA transporters), was sufficient to trigger synaptic release of both ACh and GABA from starburst cells, we used flash photolysis to uncage Ca^{2+} from DM-nitrophen, which was introduced into the presynaptic cell via a whole-cell patch pipette. With the presynaptic starburst cell voltage clamped constantly at -70 mV, a UV flash (1 ms long) evoked outward synaptic currents in the postsynaptic starburst cell voltage clamped at $+45$ mV, indicating direct Ca^{2+}-evoked GABA release from the presynaptic starburst cell (Figure 6A1). Similar UV flashes also evoked inward postsynaptic currents at -70 mV (E_{Cl}), confirming the Ca^{2+} dependency of ACh release (Figure 6A2). As a control, UV flashes without DM-nitrophen did not show any effect on starburst cells (Figure 6A3) (also note that photoreceptors in perinatal rabbit were too immature to respond to light). Importantly, when we repeated the above Ca^{2+} uncaging experiments in the presence of Cd^{2+}, we still found that the postsynaptic starburst cell responded with inward nicotinic synaptic currents at -70 mV and outward GABAergic synaptic currents at $+45$ mV (n = 3) (Figure 6B). Because Cd^{2+} should have blocked Ca^{2+}-dependent release from all cells in the retina, except the presynaptic starburst cell loaded with DM-nitrophen, this result clearly demonstrated the presence of *monosynaptic* neurotransmission between starburst cells and unequivocally confirmed the above conclusion of a Ca^{2+}-dependent corelease of ACh and GABA from a single starburst cell.

The vesicular mechanism of GABA release from starburst cells was also evident from the quantal nature of the postsynaptic currents. Figures 7A1–7A3 show postsynaptic GABA quantal currents evoked by a presynaptic voltage step during a paired recording from E30 starburst cells. While the release probability varied with the level of presynaptic depolarization (Figures 7A1 and 7A2), the postsynaptic unitary quantal responses were similar, showing an average amplitude of 25 pA at $+45$ mV and a biexponential decay phase (time constants 6.3 and 15.3 ms) with a half-decay time of 11 ms (Figure 7A3). This average single quantal response closely matched the miniature synaptic currents (Figure 7A5) recorded from the same cell during spontaneous retinal waves (Figure 7A4). Similarly, unitary quantal events could also be resolved from some paired recordings from >P21 starburst cells (Figure 7B). In most cases, however, the postsynaptic responses contained a large number of multiquantal events, which rendered detailed quantal analysis difficult.

In contrast, the nicotinic postsynaptic responses in perinatal starburst cells usually appeared as bursts of superimposed smaller events, making it difficult to resolve single quantal responses (Figure 8A). Although some postsynaptic nicotinic responses appeared shortly after the onset of a presynaptic voltage pulse (e.g., Figure 2A), the overall waveform of the postsynaptic nicotinic response often had a slow rise time (Figure 8A), which resembled the waveform of spontaneous nicotinic inputs to starburst cells during early retinal waves (Figure 8B). The slow kinetics of the nicotinic synaptic transmission between starburst cells appeared to be due, in a large part, to the kinetics of presynaptic Ca^{2+} entry and the Ca^{2+} dynamics at presynaptic release sites, because the synaptic response to flash photolysis was very fast (Figures 6A and 6B).

The release of GABA from starburst cells was often prolonged, lasting up to a few seconds after the termination of a depolarizing voltage step (Figure 8C1), perhaps, as a result of a prolonged Ca^{2+} elevation at the release sites. This prolonged GABA release might be important for lateral inhibition during visual processing, for example, by providing a sustained inhibition of a subsequent excitatory input, a mechanism that is essential for direction selectivity (Borg-Graham, 2001; Taylor and Vaney, 2003), especially in ON DS ganglion cells which are sensitive to slow motion (Oyster et al., 1972; Amthor et al., 1989; He and Masland, 1998). To show that starburst cells did receive prolonged GABAergic inhibitory inputs during light stimulation, the same postsynaptic starburst cell shown in Figure 8C1 was held at the cation reversal potential (0 mV) and stimulated with full-field light in the presence of 2 μM strychnine. The repetitive outward synaptic currents in this cell (Figure 8C2) indicated a prolonged GABAergic input following the light flash. Given the strong GABAeric interactions among starburst cells (Figure 8C1), it is conceivable that a significant portion of this light-evoked inhibitory input came directly from other starburst cells, although other GABAergic amacrine cell types might also have a contribution. The detailed mechanism of synaptic interactions between starburst cells during visual processing is still under investigation.

Discussions

The present study resulted in four new findings. (1) We demonstrated at a synaptic level the Ca^{2+}-dependent corelease of ACh and GABA from a single starburst cell. (2) We identified a network of mutually excitatory starburst cells and proved that recurrent excitation in this network mediates the propagation of early spontaneous retinal waves. (3) We discovered a developmental loss of the early nicotinic synapses between starburst cells that occurred concomitantly with a switch from excitatory to inhibitory $GABA_{A/C}$ actions in the IPL. (4) We found reciprocal GABAergic interactions between mature starburst cells and detected lateral inhibition of

component, revealing a light-evoked GABAergic inhibition. (D1) Dual recording from a starburst pair, showing outward postsynaptic currents in cell 1 ($V_h = -15$ mV) in response to a voltage pulse (-70 to 0 mV, top trace) applied to cell 2. (D2) Responses of the same starburst pair to a center illumination (100 μm in diameter, top trace). Cell 2 ($V_h = -70$ mV) responded with a delayed inward current, presumably mediated by glutamate, whereas the response of cell 1 ($V_h = -15$ mV) consisted of an initial inward current (presumably glutamatergic), followed by an outward current, presumably mediated by GABA and glycine. (D3) Simultaneous light stimulation and step depolarization of cell 2 resulted in the light response of cell 1 being shifted outward, indicating a GABAergic inhibition of the light response in cell 1 exerted by cell 2. Dashed lines indicate the level of holding current without stimulation.
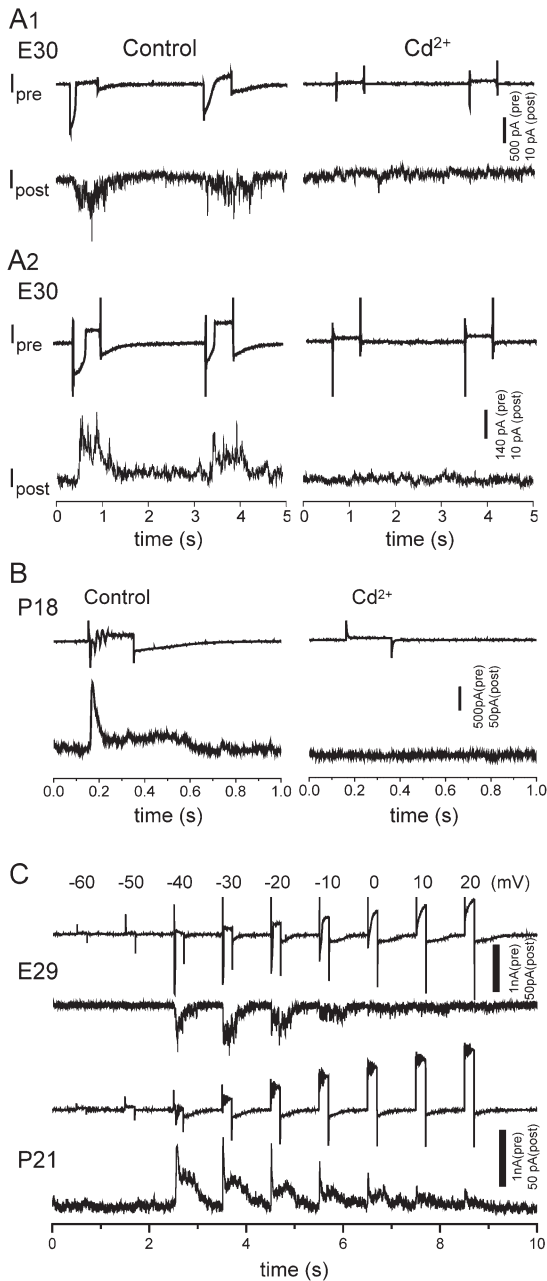
A1
E30   Control   Cd²⁺
I_pre

I_post

A2
E30
I_pre

I_post

0   1   2   3   4   5   0   1   2   3   4   5
time (s)   time (s)

B
P18   Control   Cd²⁺

0.0 0.2 0.4 0.6 0.8 1.0   0.0 0.2 0.4 0.6 0.8 1.0
time (s)   time (s)

C   -60 -50 -40 -30 -20 -10   0   10   20 (mV)

E29

P21

0   2   4   6   8   10
time (s)

Figure 5. Ca²⁺-Dependent Release of ACh and GABA by Starburst Cells

(A1) Dual voltage-clamp recording from an E30 starburst cell pair. Presynaptic depolarization from −70 to 0 mV (left) and from −70 to 15 mV (right) elicited in the presynaptic cell a series of voltage- and Ca²⁺-activated currents (I_pre), including Na⁺ currents, Ca²⁺ currents, Ca²⁺-activated currents, small residual K⁺ currents, and leak currents. The postsynaptic starburst cell (voltage clamped at −70 mV) responded with inward synaptic currents (I_post). Cd²⁺ (0.5 mM) blocked presynaptic Ca²⁺ and Ca²⁺-activated currents and abolished postsynaptic currents.
(A2) Dual recording from another E30 starburst cell pair under the same condition as in (A1), except that the postsynaptic starburst cell was voltage clamped at +45 mV, showing outward (GABA_A) postsynaptic currents which were also blocked by Cd²⁺ (0.5 mM).
(B) Dual recording from a P18 starburst cell pair, showing presynaptic voltage-activated currents (upper traces) in response to a voltage step (−70 to −30 mV) and postsynaptic response (V_h = +45 mV,

starburst cell light response by a single neighboring starburst cell.

The Role of Recurrent Starburst Network Excitation in Early Retinal Waves

Our results demonstrated that the starburst network was wired together via nicotinic and GABAergic synapses during early development and that the essential synaptic input to starburst cells during the early retinal wave was from the starburst network itself, not from other cell types. These two findings, together with the result that the early retinal wave in the rabbit retina relies critically on nicotinic neurotransmission (Zhou and Zhao, 2000), provide strong evidence for the hypothesis that recurrent excitation within the starburst network mediates the early retinal wave. Our data suggest that reciprocal nicotinic communication among starburst cells functions to amplify, synchronize, and propagate the spontaneous activity within the starburst network, although the mechanism underlying the initiation of rhythmic spontaneous activity remains to be elucidated. Since most ganglion cells receive a rhythmic nicotinic drive during early retinal waves (Feller et al., 1996), the correlated release of ACh from starburst cells may have a spatially broad action in the inner plexiform layer (IPL) and drive most, if not all, other cells that send processes to the IPL. This seems possible because the IPL is very thin at this early stage, and young starburst cells have numerous filopodia pointing away from the strata occupied by the main starburst branches (Figure 3E), as confirmed by the diffused ChAT immunoreactivity in rabbit (A. Ahmad and Z.J.Z., unpublished data), ferret (Feller et al., 1996), and rat (Kim et al., 2000). It is also possible that ACh may diffuse a distance to act on more distant target cells.

We showed that the massive nicotinic interaction among starburst cells was transient and diminished rapidly during the first postnatal week. This result explains, at least in part, why the circuitry mediating retinal waves switched from a nicotinic to a glutamatergic system in the rabbit retina as development proceeded (Zhou and Zhao, 2000). Concomitant with this drastic loss of nicotinic synapses between starburst cells, ionotropic GABAergic actions in the IPL also switched from excitation to inhibition. The GABAergic inhibition during the late-stage spontaneous wave is believed to play a role in the weakening and final disappearance of the waves in rabbit (Syed et al., 2004) and turtle (Sernagor et al., 2003).

The Development of Starburst Network Excitability

The dramatic loss of nAChR on starburst cells before eye opening suggests that the early form of reciprocal

lower traces) in a P18 starburst cell pair in the presence of 40 μM CNQX. Cd²⁺ (0.5 mM) effectively blocked the presynaptic Ca²⁺ and Ca²⁺-activated currents and the postsynaptic GABA currents.
(C) Dual recording of presynaptic voltage-activated currents (test potentials indicated on the top, V_h = −70 mV) and postsynaptic nicotinic (upper, V_h = −70 mV) and GABA (lower, V_h = +45 mV) responses from a P21 starburst cell, showing a correspondence between the presynaptic depolarization level and the postsynaptic response.
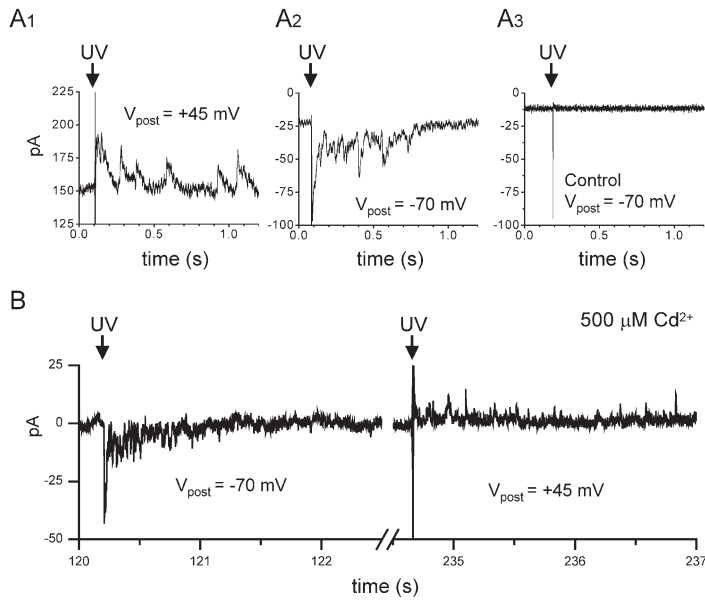
Figure 6. Flash Photolysis and Quantal Responses

(A1) Flash photolysis (1 ms duration, indicated by arrow) of DM-nitrophen, which was dialyzed into a presynaptic starburst cell ($V_h = -70$ mV) through a patch pipette, evoked fast outward synaptic currents from a postsynaptic starburst cell ($V_h = +45$ mV) under dual voltage clamp in an E30 retina.

(A2) A similar recording from another pair of E30 starburst cells (both voltage clamped at -70 mV), showing UV-evoked inward postsynaptic currents.

(A3) The same UV flash did not elicit any synaptic response in a pair of DM-nitrophen-free starburst cells ($V_h = -70$ mV). The fast spike at the onset of the UV flash is stimulation artifact due to voltage discharge.

(B) Flash photolysis in the presence of 0.5 mM Cd^{2+} evoked inward and outward postsynaptic responses (recorded at a postsynaptic V_h of -70 mV and $+45$ mV, respectively) from an E30 starburst cell pair. The presynaptic cell was loaded with DM-nitrophen and voltage clamped at -70 mV.

nicotinic excitation among starburst cells may be deleterious to visual function. Although we cannot be sure how these reciprocal excitatory synapses, if persisted to adulthood, would affect mature network, it seems plausible that the dismantling of these early positive-feedback synapses may play an important role in the transformation of starburst network excitability. It is well known that many neural networks are hyperexcitatory (epileptic) during early development and then transform to a stable (nonepileptic) state as the network matures. The current theory on such a transformation is based primarily on the delayed expression of K-Cl cotransporters (Rivera et al., 1999), which results in a negative shift of the reversal potential of GABA- and glycine-gated
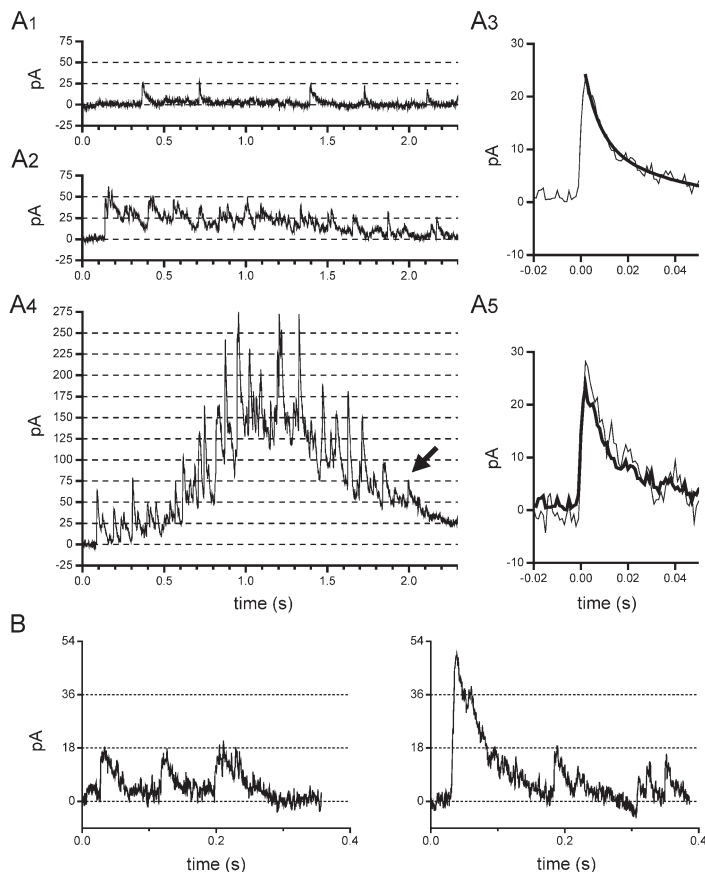

Figure 7. Quantal GABA Currents in Starburst Cells

(A1) Dual voltage-clamp recording from a pair of E30 starburst cells, showing postsynaptic unitary quantal currents ($V_h = +45$ mV) in response to a presynaptic voltage step from -70 to $+40$ mV.

(A2) Postsynaptic currents from the same cell pair in (A1) in response to a presynaptic voltage step from -70 to $+10$ mV, showing numerous multiquantal events ($V_h = +45$ mV) and a unitary amplitude similar to that in (A1).

(A3) An average of the five unitary quantal events in (A1) (thin line). The decay time course is biexponential (thick line), with time constants 6.3 and 15.3 ms. The half-decay time is 11 ms.

(A4) Synaptic currents during a spontaneous retinal wave recorded from the same postsynaptic cell as in (A1)–(A3) ($V_h = +45$mV).

(A5) A unitary synaptic current (thin line) from (A4) (indicated by arrow) was compared with the average quantal event (thick line) in (A3), showing a close match.

(B) Postsynaptic currents ($V_h = +45$ mV) evoked by presynaptic depolarization from -70 to -20 mV (left) and from -70 to $+10$ mV (right) during a paired recording of starburst cells in a P29 retina.
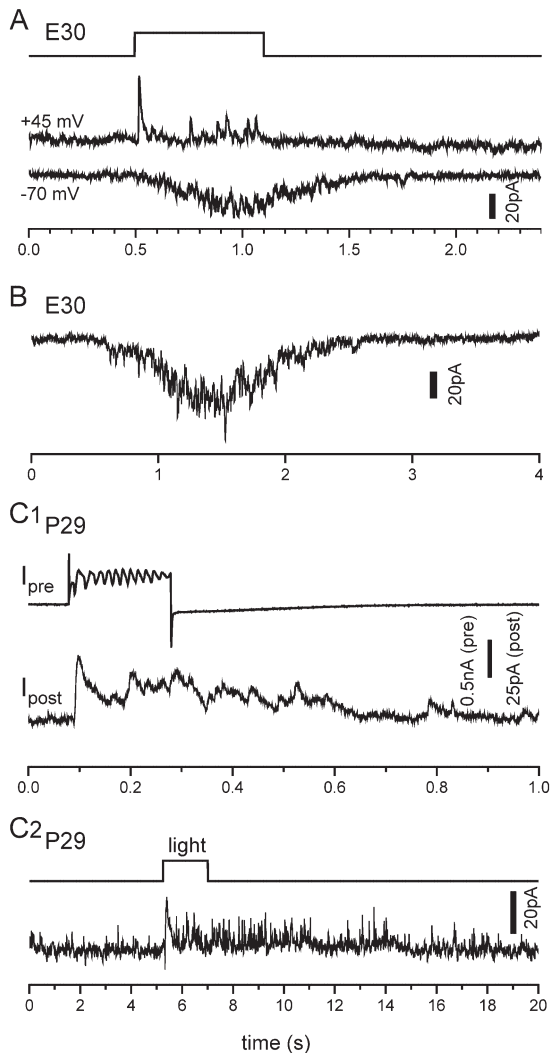
ever, the early spontaneous wave in the developing mammalian retina is unusual in that it is mediated by ACh via a network of reciprocal nicotinic synapses as demonstrated in this study. How does an intrinsically unstable nicotinic network transform its excitability during development? There appear to be two conceptual solutions: (1) the intrinsic nicotinic instability is permissible and suppressible by GABAergic and glycinergic inhibition among starburst and other amacrine cells in the mature retina; (2) such instability is deleterious to vision and should be abolished during development. Our results clearly show that the second solution is the one adopted by retinal development, suggesting that mature retinal circuits are designed specifically to avoid intrinsic instability. Thus, the general mechanism for the transformation of network excitability during development may include both a switch of GABA and glycine excitability and a dismantling of early positive-feedback synapses. In addition to these two scenarios, developmental switches in neurotransmitter and postsynaptic receptor phenotypes have also been reported (Guidry and Landis, 1998; Asmus et al., 2000; Joshi and Wang, 2002), providing yet another way of modulation, if not complete switch, of network excitability.

Mutual GABAergic Inhibition and the Function of Starburst Cells during Visual Processing

Recent advances in the study of direction selectivity indicate a critical role of asymmetric interactions at the level of starburst cells, particularly with respect to the centrifugally preferred Ca^{2+} response of individual starburst processes to moving stimuli (Euler et al., 2002) and the asymmetric GABAergic interactions between starburst and DS ganglion cells (Fried et al., 2002). One of the remaining key questions is whether the centrifugally preferred response in starburst processes is generated by intrinsic starburst cell properties, by network (synaptic) interactions, or a combination of the two. Theoretical models have previously proposed a prominent role of starburst-starburst interaction in the DS mechanism (Borg-Graham, 2001), but there has been no physiological evidence for such synaptic interactions. Although synaptic contacts between adult starburst processes have been seen at the electron-microscopic level (Brandon, 1987; Millar and Morgan, 1987; Mariani and Hersh, 1988; Famiglietti, 1991; Firth et al., 2003), the occurrence of these contacts has been rare (Famiglietti, 1991), and the neurochemical identity of such contacts has remained unclear. Our recordings now provide physiological evidence for direct GABAergic synaptic interactions between mature starburst cells, suggesting that most of the synaptic contacts between starburst cells are GABAergic. We also showed that starburst cells inhibit each other during light stimulation. Our finding of the Ca^{2+}-dependent vesicular GABA release indicates that the GABA release sites are restricted to the distal varicose zones where synaptic vesicles are localized, consistent with the notion that the distal zones are important processing units of starburst cells. Unlike the previous view that local starburst processing units mainly feed forward to ganglion cells, our data demonstrate that these processing units also exert mutual lateral inhibition among overlapping starburst cells, thus providing

Figure 8. Kinetics of Nicotinic and GABA$_A$ Receptor-Mediated Synaptic Transmission in Starburst Cells

(A) Comparison of synaptic GABA (recorded at +45 mV, middle trace) and ACh (recorded at −70 mV, bottom trace) currents in a postsynaptic starburst cell in response to a voltage pulse (from −70 to 0 mV, top trace) applied to a presynaptic starburst cell under dual patch-clamp recording in an E30 retina. The GABA response consisted of multiple quantal events and appeared quickly after the onset of the voltage step, whereas the nicotinic response appeared as a smoother current with a much slower rise time.
(B) Spontaneous synaptic input to an E30 starburst cell (V_h = −70mV) during a retinal wave, showing a waveform similar to that of nicotinic postsynaptic currents in (A) (bottom trace).
(C1) Dual recording from a P29 starburst pair, showing presynaptic voltage-activated currents in response to a step depolarization (−70 to −10 mV) and prolonged postsynaptic GABAergic responses (recorded at +45 mV).
(C2) Response of the same postsynaptic starburst cell as in (C1) (V_h = 0 mV) to a full-field light flash in the presence of strychnine (2 μM). The repetitive outward synaptic currents indicate prolonged, light-induced GABAergic inputs.

currents (Ben-Ari, 2002). This theory has worked very well in nearly all previously known cases, because most of the spontaneous excitation in these early networks is thought to be driven by GABA or glycine inputs. How-

dynamic and complex lateral interactions prior to DS ganglion cells. Because DS is such a robust and fundamental phenomenon observable under a wide range of stimulation conditions, it is conceivable that the formation of DS responses may involve multiple levels of synaptic interactions and several synergistic network mechanisms. We propose that the GABAergic inhibition among starburst cells, especially in local distal processes, may provide a new level of network computation to enhance the centrifugal-centripetal asymmetry in GABA release from starburst cells. GABAergic starburst-starburst interactions may also provide an important mechanism for lateral inhibition.

Our finding of the Ca^{2+} dependence of GABA release from starburst cells has another direct implication to the mechanism of direction selectivity. Previously, the centrifugally preferred Ca^{2+} response in starburst distal processes was thought as an indication of local membrane depolarization, which would trigger transporter-mediated GABA release (Euler et al., 2002). Given the Ca^{2+} dependency of GABA release found in this study, the preferred Ca^{2+} response to centrifugal motion (Euler et al., 2002) now indicates a much stronger asymmetric GABA release than previously thought, because of the supralinear dependence of vesicular release on Ca^{2+} (Ca^{2+} cooperativity) (Dodge and Rahamimoff, 1967; Sakaba and Neher, 2001).

Corelease of ACh and GABA by Starburst Cells

Starburst cells are one of the few known neuron types in the CNS that colocalize and corelease two fast neurotransmitters (Jonas et al., 1998; Jo and Schlichter, 1999; Tsen et al., 2000). Our finding that a single starburst cell releases both ACh and GABA extends the previous autoradiographic results (O'Malley and Masland, 1989) to the synaptic level. With combined dual patch clamp and flash photolysis, we further demonstrated that both cholinergic and GABAergic communications between developing starburst cells were monosynaptic. Our conclusion of a Ca^{2+}-dependent vesicular GABA release mechanism in starburst cells was based on three results: Cd^{2+} blocked the release; uncaging Ca^{2+} evoked the release; and postsynaptic quantal currents. Our data, however, do not exclude the possible presence of a low-level Ca^{2+}-independent component of GABA release in extrasynaptic/nonsynaptic regions.

Because it is well established that starburst cells release ACh in the adult retina (Masland and Livingstone, 1976), mature starburst cells are expected to form functional nicotinic synapses with other cell types. We did not detect any nicotinic synaptic currents between mature starburst cells (even in the presence of neostigmine, n = 2). Given that the response of starburst cells to 1 mM DMPP puff declined dramatically from ~2 nA at E29 to ~30 pA in adult, the lack of a detectable synaptic response between mature starburst cells seems expected and is consistent with a previous imaging study showing no Ca^{2+} response to nicotine from adult starburst cells (Baldridge, 1996). However, because mature starburst cells still gave small responses to puffs of DMPP or ACh (in the presence of NS) (Figures 3C and 3D), it remains a possibility that limited nicotinic interactions may exist on distal processes between mature starburst cells or that a low level of nicotinic autoreceptors may be present. It is also possible that a distal response to DMPP puff was not fully resolved at the soma due to a lack of adequate space clamp at the thin distal processes. On the other hand, because we could detect starburst responses to GABA puffs at distal processes and resolve glutamate-mediated responses to spot illumination at the distal processes (S.L. and Z.J.Z., unpublished data) as previously reported (Peters and Masland, 1996), we think that the level of nicotinic receptor expression in adult starburst cells must be very low. A low level of immunoreactivity to nicotinic receptor antibodies has been reported previously for a subset (predominantly in central retina) of cholinergic cells in the GCL of the adult rabbit retina (Keyser et al., 2000). The function of these low-level nicotinic receptors and small nicotinic currents in adult starburst cells is currently unclear. Here, we speculate three possibilities. First, the small amount of nicotinic response from adult starburst cells may indicate the presence of receptors left over from the early stage of development. This would explain why only a small, inconsistent population of adult starburst cells were found to be weakly immunoreactive to nicotinic antibodies (Keyser et al., 2000). However, given the many examples of tight regulation of protein expression during development, this possibility seems unlikely. Second, a limited number of nicotinic synapses may be present locally between distal dendrites of starburst cells, but synaptic transmission at these synapses may be too small to be detected at the soma, due to either poor space clamp or a lack of optimal stimulation condition (e.g., a lack of coordinated excitation in many cofasciculated starburst cells). These local nicotinic synapses might be few in number, but could be functionally important, especially for local signaling (such as for direction selectivity). Third, a low level of nicotinic transmission (either synaptic or nonsynaptic) may exist between mature starburst cells, but only produces a small electric change in the basal activity of the cell, which might be difficult to identify during paired recordings. Such a cholinergic action could play a role in modulating the response sensitivity of starburst cells, similar to that proposed previously for ganglion cells (Ariel and Daw, 1982).

Our results showed that the corelease of ACh and GABA by starburst cells is functionally significant. In the developing retina, we now prove that ACh release from starburst cells is critical for retinal wave formation. According to our recent classification (Syed et al., 2004), stage II retinal waves (between the ages E24 and P2) are mediated by nicotinic receptors, and stage III waves (P4–P8) by glutamate and muscarinic receptors (Zhou and Zhao, 2000; Syed et al., 2004). The release of GABA by starburst cells also provides a significant synaptic input to starburst and other cells during retinal waves. Blocking GABA receptors dramatically increased the frequency, intensity, and propagation of stage III waves (Syed et al., 2004). However, it is currently unclear whether GABA plays a significant role in stage II retinal waves. It has been suggested that the release of GABA during stage II waves may be important for the maturation of the GABA system in the inner retina, especially with respect to K-Cl cotransporter expression (E. Sernagor et al., 2003, Soc. Neurosci., abstract).

In the adult retina, it is well accepted that GABA release from starburst cells is critical for direction selectivity (Fried et al., 2002). However, the exact mechanism and function of cholinergic interaction in the mature retina are poorly understood, even though ACh has been shown to influence the response of ganglion cells (Ariel and Daw, 1982), including DS ganglion cells (Amthor et al., 1996; He and Masland, 1997; Chiao and Masland, 2002). It remains a puzzle that, while starburst and DS cell processes cofasciculate immensely, direct cholinergic input to DS ganglion cells has so far remained elusive (Fried et al., 2002). It is also not clear whether ACh, once released, only functions locally near its release sites or acts broadly over a long range through diffusion. Thus, the exact synaptic mechanism and function of starburst cells remain an intriguing question for future studies. What we can tell from the present study is that the ability of starburst cells to release both ACh and GABA, together with a dynamic developmental modification of the network excitability and connectivity, allows the starburst network to play diverse functional roles in both visual development and visual function.

Experimental Procedures

Dual Patch-Clamp Recording from Starburst Cells in Flat-Mount Rabbit Retina

Retinal flat-mounts were made from New Zealand White rabbits aged E29 to adult (~2.5 kg) as described (Zhou, 1998). All procedures involving the use of animals were done according to NIH guidelines. For patch-clamp recording, a piece of retina was placed in a recording chamber and held to the bottom of the chamber, sclera side down, by a nylon mesh glued to a platinum ring. The recording chamber was continuously superfused (3–4 ml/min) with Ames medium (Ames and Nesbett, 1981) at 34°C–37°C. Displaced starburst cells (the population of starburst cells with soma located in the GCL) were targeted for recording based on their 8–10 μm soma diameter and proximity to the IPL. Definitive identification of cell type was made morphologically with epifluorescence after whole-cell recording with pipettes containing Lucifer yellow. Müller cell endfeet and extracellular connective tissues that covered the neurons in the ganglion cell layer were removed mechanically with a large-tip patch pipette or a pair of fine forceps. Patch-clamp recordings were made in the whole-cell configuration using EPC9-2 (Heka Elektronic, Lambrecht, Germany) or Axopatch 700A (Axon Instruments, Inc., Union City, CA) amplifiers under a 40× or 60× water-immersion objective lens on a fixed-stage, upright fluorescence microscope (BX50WI, Olympus USA, NY). Liquid junction potential was corrected as previously described (Fenwick et al., 1982). Data from continuous recordings were low-pass filtered at 2 kHz (f_c), digitized at 10 kHz, and stored on computer hard drive by Power Lab (AD Instruments, Castle Hill, Australia). Data acquisition and analysis were done with the software Pulse (Heka), pCLAMP 8 (Axon Instruments), Chart 5 (AD Instruments), and Origin 6 (MicroCal Software Inc., Northampton, MA). Original voltage-gated currents were shown in figures without leak subtraction.

Light Stimulation, Flash Photolysis, and Ca^{2+} Imaging

Light responses were recorded under whole-cell patch clamp in light-adapted retinas from P10–P29 rabbits. The retina was allowed to dark adapt for 5–10 min before being stimulated by full-field or spot (100 μm diameter) flashes of light from a 100 W halogen lamp through the microscope condenser or from a 75 W Xenon lamp (band-pass filtered at 450–550) through a 60× water-immersion objective lens (NA = 0.9) and a series of neutral density filters (3%–30% transmission). The timing of the light flash was controlled by the pClamp 8 software through a Uniblitz shutter (Vincent Associates, Rochester, NY).

Flash photolysis was done using a xenon flash lamp (Model JML-C2, Rapp Optoelectronic, Hamburg, Germany) attached to the epifluorescence port of the microscope via a quartz optic fiber. DM-nitrophen (10 mM) was loaded with Ca^{2+} (to ~80%) in the pipette solution (see below). UV flashes (1 ms duration) were delivered to the retina through a 40× water-immersion objective lens (NA = 0.8). The timing of the flash was controlled by the Pulse software (Heka).

Ca^{2+} imaging was made from putative displaced starburst cells with a cooled CCD camera (Cascade, Roper Scientific, Princeton, NJ) through 40× water-immersion lens (NA = 0.8), after the retina was loaded with Fura-2AM as described (Zhou and Zhao, 2000). The cell morphology was confirmed at the end of imaging, with intracellular Lucifer yellow injection.

Solutions

All recordings were made in Ames medium (saturated with 95% O$_2$/ 5% CO$_2$), except when testing the effect of Cd^{2+} (0.3–1 mM), in which case the extracellular solution (modified Ames) contained 119 mM NaCl, 2.5 mM KCl, 1.3 mM MgCl$_2$, 2.5 mM CaCl$_2$, 20 mM HEPES, 10 mM glucose, and 0.1 mM ascorbic acid (pH = 7.4) and was bubbled with O$_2$. The intracellular (pipette) solution contained 110 mM CsMeSO$_4$, 5 mM NaCl, 0.5 mM CaCl$_2$, 2 mM MgCl$_2$, 5 mM EGTA, 2 mM adenosine 5'-triphosphate (disodium salt), 0.5 mM guanosine 5'-triphosphate (trisodium salt), 10 mM HEPES, and 2 mM ascorbate (pH 7.2, with CsOH) and was supplemented with 0.1%–0.3% (w/v) Lucifer yellow (molecular Probes, Eugine, OR). MgCl$_2$ and EGTA were omitted from the pipette solution when DM-nitrophen was supplemented. Nicotinic and GABAergic agonists were puffed to the cells using Picospritzer II (General Valve, Fairfield, NJ). All other drugs (Sigma, St. Louse, MO) were applied via bath perfusion.

References

Ames, A., and Nesbett, F.B. (1981). In vitro retina as an experimental model of the central nervous system. J. Neurochem. *37*, 867–877.

Amthor, F.R., Takahashi, E.S., and Oyster, C.W. (1989). Morphologies of rabbit retinal ganglion cells with complex receptive fields. J. Comp. Neurol. *280*, 97–121.

Amthor, F.R., Grzywacz, N.M., and Merwine, D.K. (1996). Extra-receptive-field motion facilitation in on-off directionally selective ganglion cells of the rabbit retina. Vis. Neurosci. *13*, 303–309.

Amthor, F.R., Keyser, K.T., and Dmitrieva, N.A. (2002). Effects of the destruction of starburst-cholinergic amacrine cells by the toxin AF64A on rabbit retinal directional selectivity. Vis. Neurosci. *19*, 495–509.

Ariel, M., and Daw, N.W. (1982). Effects of cholinergic drugs on receptive field properties of rabbit retinal ganglion cells. J. Physiol. (Lond). *324*, 135–160.

Asmus, S.E., Parsons, S., and Landis, S.C. (2000). Developmental changes in the transmitter properties of sympathetic neurons that innervate the periosteum. J. Neurosci. *20*, 1495–1504.

Baldridge, W.H. (1996). Optical recordings of the effects of cholinergic ligands on neurons in the ganglion cell layer of mammalian retina. J. Neurosci. *16*, 5060–5072.

Ben-Ari, Y. (2002). Excitatory actions of gaba during development: the nature of the nurture. Nat. Rev. Neurosci. *3*, 728–739.

Borg-Graham, L.J. (2001). The computation of directional selectivity in the retina occurs presynaptic to the ganglion cell. Nat. Neurosci. *4*, 176–183.

Brandon, C. (1987). Cholinergic neurons in the rabbit retina: dendritic branching and ultrastructural connectivity. Brain Res. *426*, 119–130.

Brecha, N., Johnson, D., Peichl, L., and Wassle, H. (1988). Cholinergic amacrine cells of the rabbit retina contain glutamate decarboxylase and gamma-aminobutyrate immunoreactivity. Proc. Natl. Acad. Sci. USA *85*, 6187–6191.

Chiao, C.C., and Masland, R.H. (2002). Starburst cells nondirectionally facilitate the responses of direction-selective retinal ganglion cells. J. Neurosci. *22*, 10509–10513.

Dodge, F.A., Jr., and Rahamimoff, R. (1967). Co-operative action a calcium ions in transmitter release at the neuromuscular junction. J. Physiol. *193*, 419–432.

Euler, T., Detwiler, P.B., and Denk, W. (2002). Directionally selective calcium signals in dendrites of starburst amacrine cells. Nature *418*, 845–852.

Famiglietti, E.V. (1985). Starburst amacrine cells: morphological constancy and systematic variation in the anisotropic field of rabbit retinal neurons. J. Neurosci. *5*, 562–577.

Famiglietti, E.V. (1991). Synaptic organization of starburst amacrine cells in rabbit retina: analysis of serial thin sections by electron microscopy and graphic reconstruction. J. Comp. Neurol. *309*, 40–70.

Feller, M.B. (1999). Spontaneous correlated activity in developing neural circuits. Neuron *22*, 653–656.

Feller, M.B., Wellis, D.P., Stellwagen, D., Werblin, F.S., and Shatz, C.J. (1996). Requirement for cholinergic synaptic transmission in the propagation of spontaneous retinal waves. Science *272*, 1182–1187.

Feller, M.B., Butts, D.A., Aaron, H.L., Rokhsar, D.S., and Shatz, C.J. (1997). Dynamic processes shape spatiotemporal properties of retinal waves. Neuron *19*, 293–306.

Fenwick, E.M., Marty, A., and Neher, E. (1982). A patch-clamp study of bovine chromaffin cells and of their sensitivity to acetylcholine. J. Physiol. (Lond). *331*, 577–597.

Firth, S.I., Li, W., Massey, S.C., and Marshak, D.W. (2003). AMPA receptors mediate acetylcholine release from starburst amacrine cells in the rabbit retina. J. Comp. Neurol. *466*, 80–90.

Fried, S.I., Munch, T.A., and Werblin, F.S. (2002). Mechanisms and circuitry underlying directional selectivity in the retina. Nature *420*, 411–414.

Guidry, G.L., and Landis, S.C. (1998). Developmental regulation of neurotransmitters in sympathetic neurons. Adv. Pharmacol. *42*, 895–898.

He, S., and Masland, R.H. (1997). Retinal direction selectivity after targeted laser ablation of starburst amacrine cells. Nature *389*, 378–382.

He, S., and Masland, R.H. (1998). ON direction-selective ganglion cells in the rabbit retina: dendritic morphology and pattern of fasciculation. Vis. Neurosci. *15*, 369–375.

Hutchins, J.B., Bernanke, J.M., and Jefferson, V.E. (1995). Acetylcholinesterase in the developing ferret retina. Exp. Eye Res. *60*, 113–125.

Jo, Y.H., and Schlichter, R. (1999). Synaptic corelease of ATP and GABA in cultured spinal neurons. Nat. Neurosci. *2*, 241–245.

Jonas, P., Bischofberger, J., and Sandkuhler, J. (1998). Corelease of two fast neurotransmitters at a central synapse. Science *281*, 419–424.

Joshi, I., and Wang, L.Y. (2002). Developmental profiles of glutamate receptors and synaptic transmission at a single synapse in the mouse auditory brainstem. J. Physiol. *540*, 861–873.

Katz, L.C., and Shatz, C.J. (1996). Synaptic activity and the construction of cortical circuits. Science *274*, 1133–1138.

Keyser, K.T., MacNeil, M.A., Dmitrieva, N., Wang, F., Masland, R.H., and Lindstrom, J.M. (2000). Amacrine, ganglion, and displaced amacrine cells in the rabbit retina express nicotinic acetylcholine receptors. Vis. Neurosci. *17*, 743–752.

Kim, I.B., Lee, E.J., Kim, M.K., Park, D.K., and Chun, M.H. (2000). Choline acetyltransferase-immunoreactive neurons in the developing rat retina. J. Comp. Neurol. *427*, 604–616.

Kosaka, T., Tauchi, M., and Dahl, J.L. (1988). Cholinergic neurons containing GABA-like and/or glutamic acid decarboxylase-like immunoreactivities in various brain regions of the rat. Exp. Brain Res. *70*, 605–617.

MacNeil, M.A., Heussy, J.K., Dacheux, R.F., Raviola, E., and Masland, R.H. (1999). The shapes and numbers of amacrine cells: matching of photofilled with Golgi-stained cells in the rabbit retina and comparison with other mammalian species. J. Comp. Neurol. *413*, 305–326.

Mariani, A.P., and Hersh, L.B. (1988). Synaptic organization of cholinergic amacrine cells in the rhesus monkey retina. J. Comp. Neurol. *267*, 269–280.

Masland, R.H. (1977). Maturation of function in the developing rabbit retina. J. Comp. Neurol. *175*, 275–286.

Masland, R.H., and Livingstone, C.J. (1976). Effect of stimulation with light on synthesis and release of acetylcholine by an isolated mammalian retina. J. Neurophysiol. *39*, 1210–1219.

Millar, T.J., and Morgan, I.G. (1987). Cholinergic amacrine cells in the rabbit retina synapse onto other cholinergic amacrine cells. Neurosci. Lett. *74*, 281–285.

O'Donovan, M.J. (1999). The origin of spontaneous activity in developing networks of the vertebrate nervous system. Curr. Opin. Neurobiol. *9*, 94–104.

O'Malley, D.M., and Masland, R.H. (1989). Co-release of acetylcholine and gamma-aminobutyric acid by a retinal neuron. Proc. Natl. Acad. Sci. USA *86*, 3414–3418.

O'Malley, D.M., Sandell, J.H., and Masland, R.H. (1992). Co-release of acetylcholine and GABA by the starburst amacrine cells. J. Neurosci. *12*, 1394–1408.

Oyster, C.W., Takahashi, E., and Collewijn, H. (1972). Direction-selective retinal ganglion cells and control of optokinetic nystagmus in the rabbit. Vision Res. *12*, 183–193.

Peters, B.N., and Masland, R.H. (1996). Responses to light of starburst amacrine cells. J. Neurophysiol. *75*, 469–480.

Rivera, C., Voipio, J., Payne, J.A., Ruusuvuori, E., Lahtinen, H., Lamsa, K., Pirvola, U., Saarma, M., and Kaila, K. (1999). The K+/Cl-co-transporter KCC2 renders GABA hyperpolarizing during neuronal maturation. Nature *397*, 251–255.

Rockhill, R.L., Euler, T., and Masland, R.H. (2000). Spatial order within but not between types of retinal neurons. Proc. Natl. Acad. Sci. USA *97*, 2303–2307.

Rockhill, R.L., Daly, F.J., MacNeil, M.A., Brown, S.P., and Masland, R.H. (2002). The diversity of ganglion cells in a mammalian retina. J. Neurosci. *22*, 3831–3843.

Sakaba, T., and Neher, E. (2001). Quantitative relationship between transmitter release and calcium current at the calyx of held synapse. J. Neurosci. *21*, 462–476.

Sernagor, E., Young, C., and Eglen, S.J. (2003). Developmental modulation of retinal wave dynamics: shedding light on the GABA saga. J. Neurosci. *23*, 7621–7629.

Syed, M.M., Lee, S., Zheng, J., and Zhou, Z.J. (2004). Stage-dependent dynamics and modulation of spontaneous waves in the developing rabbit retina. J. Physiol. *560*, 533–549.

Tauchi, M., and Masland, R.H. (1984). The shape and arrangement of the cholinergic neurons in the rabbit retina. Proc. R. Soc. Lond. B Biol. Sci. *223*, 101–119.

Taylor, W.R., and Vaney, D.I. (2003). New directions in retinal research. Trends Neurosci. *26*, 379–385.

Tsen, G., Williams, B., Allaire, P., Zhou, Y.D., Ikonomov, O., Kondova, I., and Jacob, M.H. (2000). Receptors with opposing functions are in postsynaptic microdomains under one presynaptic terminal. Nat. Neurosci. *3*, 126–132.

Vaney, D.I. (1984). 'Coronate' amacrine cells in the rabbit retina have the 'starburst' dendritic morphology. Proc. R. Soc. Lond. B. Biol. Sci. *220*, 501–508.

Vaney, D.I., and Young, H.M. (1988). GABA-like immunoreactivity in cholinergic amacrine cells of the rabbit retina. Brain Res. *438*, 369–373.

Vu, T.Q., Payne, J.A., and Copenhagen, D.R. (2000). Localization and developmental expression patterns of the neuronal K-Cl co-transporter (KCC2) in the rat retina. J. Neurosci. *20*, 1414–1423.

Wassle, H., and Boycott, B.B. (1991). Functional architecture of the mammalian retina. Physiol. Rev. *71*, 447–480.

Wong, R.O., and Collin, S.P. (1989). Dendritic maturation of displaced putative cholinergic amacrine cells in the rabbit retina. J. Comp. Neurol. *287*, 164–178.

Yoshida, K., Watanabe, D., Ishikane, H., Tachibana, M., Pastan, I., and Nakanishi, S. (2001). A key role of starburst amacrine cells in originating retinal directional selectivity and optokinetic eye movement. Neuron *30*, 771–780.

Zhou, Z.J. (1998). Direct participation of starburst amacrine cells in spontaneous rhythmic activities in the developing mammalian retina. J. Neurosci. *18*, 4155–4165.

Zhou, Z.J. (2001). A critical role of the strychnine-sensitive glycinergic system in spontaneous retinal waves of the developing rabbit. J. Neurosci. *21*, 5158–5168.

Zhou, Z.J., and Zhao, D. (2000). Coordinated transitions in neurotransmitter systems for the initiation and propagation of spontaneous retinal waves. J. Neurosci. *20*, 6570–6577.